

# Experimental investigation of heat transfer and exergy loss in heat exchanger with air bubble injection technique

Gurpreet Singh Sokhal<sup>1</sup>, Gurprinder Singh Dhindsa<sup>1</sup>, Kamaljit Singh Sokhal<sup>2</sup>,  
Mahyar Ghazvini<sup>3,\*</sup>, Mohsen Sharifpur<sup>4,5,\*</sup> and Milad Sadeghzadeh<sup>6</sup>

<sup>1</sup> Department of Mechanical Engineering, Chandigarh University, Gharuan, Mohali, Punjab, India

<sup>2</sup> Department of Chemical Engineering, Thapar Institute of Engineering and Technology, Patiala, Punjab, India

<sup>3</sup> Department of Ocean and Mechanical Engineering, Florida Atlantic University, 777 Glades Road, Boca Raton, FL 33431, USA

<sup>4</sup> Department of Mechanical and Aeronautical Engineering, University of Pretoria, Pretoria 0002, South Africa

<sup>5</sup> Institute of Research and Development, Duy Tan University, Da Nang 550000, Vietnam

<sup>6</sup> Department of Renewable Energy and Environmental Engineering, University of Tehran, Tehran, Iran

\*Correspondence to:

\* Mahyar Ghazvini mghazvini2020@fau.edu

\* Mohsen Sharifpur mohsen.sharifpur@up.ac.za; mohsensharifpur@duytan.edu.vn

## Abstract

The main aim of this study is to evaluate thermal performance and exergy analysis of a shell-and-tube heat exchanger with a new technique called air bubble injection. The study has been carried out with different parameters such as flow rate, fluid inlet temperature, and different air injection techniques. The air has been injected at different locations such as the inlet of pipe, throughout the pipe, and in the outer pipe of the heat exchanger. Based on the results, the performance of the heat exchanger enhances with an increase in the flow rate and the fluid inlet temperature. The exergy loss and dimensionless exergy loss increase with a rise in the flow rate. The maximum and dimensionless exergy losses are obtained at a maximum flow rate of  $3.5 \text{ l min}^{-1}$ . With the air bubble injection in the heat exchanger, it has been observed that the temperature difference increases, which leads to an increase in the exergy loss. The injecting air bubbles throughout the tube section shows that minimum dimensionless exergy is 27.49% concerning no air injection.

## Keywords

Air bubble injection; Dimensionless exergy loss; Heat transfer performance; Effectiveness

## Abbreviations

### List of symbols

$A$	Tube area, ( $\text{m}^2$ )
$C_p$	Specific heat, ( $\text{J kg}^{-1}$ )
$H$	Heat transfer coefficient ( $\text{W m}^{-2} \text{K}^{-1}$ )
$m$	Mass flow rate, ( $\text{kg s}^{-1}$ )
$Q$	Heat transfer rate, (W)
$T$	Temperature, ( $^{\circ}\text{C}$ )
$U$	Overall heat transfer coefficient, ( $\text{W m}^{-2} \text{K}^{-1}$ )

### Subscripts

Avg	Average
c	Cold fluid
h	Hot fluid
i	Inlet
m	Mean
o	Outlet
w	Wall

## Introduction

Studies have used several methods to improve the performance of the various heat exchangers, for example, introduction of baffles, turbulence, vibrating the surfaces, etc. The researchers have used active and passive methods to increase the efficiency of heat transfer devices [1,2,3,4,5,6]. During the previous decades, concerns to constrained petroleum products and enormous natural issues brought about by the continuous pattern of vitality utilization have motivated scientists to look for approaches to preserve vitality or streamline frameworks for the energy consumption [7, 8]. The improvement in the performance of heat transfer devices can be mentioned as a promising method to obviate this issue [9,10,11,12,13]. The application of nanofluids is also one technique to enhance the performance of heat transfer devices [14,15,16,17,18]; on the other hand, this is not possible to use the nanofluids in all industries due to some higher cost of operating. An active method of air or gas injection in fluids has been introduced to create the turbulence in the heat transfer devices so that more energy can be transferred, which leads to a minimum loss of energy. Jiakai et al. [19] analytically revealed an explanation for how the bubble reduces the skin friction drag in boundary layers. The study explained the behavior of bubbles over the flowing fluid, and many correlations have been tried to develop for the bubble effect. Mattson and Mahesh [20] studied analytically the effect of the bubble over different parameters under turbulent boundary layer. Through the study, it has been revealed that how bubble size affects the turbulence. Larger size bubble can form more separation in a turbulent flow while smaller size bubble just makes impacts close to the wall or the point of generation. Jacob et al. [21] explored the impact of air bubbles and revealed that the shear stress and the Reynolds stress close to the wall for two-stage streams have

been diminished with the downstream of infusion compared with the single-stage stream. Heyhat et al. [22] carried out a study to evaluate the performance and exergy loss in a double-pipe heat exchanger with air bubble injection at different flow rates and angles of the heat exchanger. They revealed that the heat transfer performance has been significantly improved with the air injection method. The exergy loss has been increased from 2% to 226% with the air bubble injection in the heat exchanger. Pourhedyat et al. [23] studied the thermal performance and exergy behavior of a vertical heat transfer device with the air bubble injection method. In the work, they have revealed that the thermal performance has been significantly improved as the air has been injected in the system. On the other hand, air injection methods also lead to the destruction of exergy while the loss of exergy with the air injection method is less as compared to the introduction of turbulators, inserts, etc. Dizaji et al. [24] conducted experiments and carried out exergy analysis on a shell-and-tube heat exchanger (placed vertically) with an air injection method to improve its thermal performance. They reported that exergy loss has been increased with an air bubble introduction in the existing method. The effectiveness of the device has been augmented by 36% with air injection as compared to without air injection method. With air injection, the number of transfer units has been increased up to four times and exergy loss has been increased from 1% to 3%. Winkel et al. [25] injected fine bubbles through porous metals in a turbulent flow and observed the effect of bubbles on different concentrations of salt in water. It has been observed that fine bubbles' effect on the thermal boundary layer is different in fresh water and salt water. The size of the bubble has been reduced with a concentration of salt and bubble size does not saturate with at low concentration of salt. It was concluded that bubble size has a significant effect on drag reduction in fresh water and salt water. Mahdi et al. [26] published a comprehensive literature review on the nanofluids used for thermosyphons in which the articles with optimum concentration of the nanofluids were used. Khorasani and Dadvand [27] performed an experiment on the air injection method in helical and coiled tube heat exchangers to analyze the performance and exergy loss in the system. The effectiveness, number of transfer units, and exergy have been evaluated at a different air flow rate, and they were compared with the heat exchanger without air injection methods. The effectiveness (actual heat transfer with respect to maximum possible heat transfer) of the device has been augmented with air injection compared to no air injection method. The exergy loss has been increased from 1.8% to 14.2% with the air injection method. The exergy loss analysis is carried out for parallel flow and counter flow configuration, and it is observed that exergy loss is more in the counter flow method. Ahmadi et al. [28] successfully optimized the use of nanofluids in micro-channels and optimized the design of the heat exchanger using the finite volume method.

Akpinar and Bicer [29] investigated the exergy loss in a double-pipe heat exchanger which has been equipped with a swirl generator. The experimentation has been carried out for turbulent flow at Reynolds number 8500–17,500. They revealed that with the swirl generator in the heat exchanger, Nusselt number had been increased up to 130% and the friction factor has been three times compared to the heat exchanger without any swirl generators. The dimensionless exergy loss for the heat exchanger equipped with the swirl generator was 1.25 times more than that without a swirl generator. Nandan and Singh [30, 31] reported in their studies that the heat transfer performance of a shell-and-tube heat exchanger is significantly enhanced with the use of air injection techniques. The air has been injected in three different locations, i.e., (1) inlet of shell side, (2) inlet of tube side, and (3)

throughout the tube. The heat transfer has been augmented up to 40% with air bubbles injections. Among the three different cases, maximum enhancement has been observed when air has been injected throughout the tube. The dimensionless exergy loss was 45% higher with air bubbles injection compared to without air injection methods. In another study, Thakur and Singh [32, 33] investigated the performance of a shell-and-tube heat exchanger with nanofluids and air bubble methods. The study has been carried out with the variation of Reynolds number (4000–24,000), nanoparticle concentrations (0–0.2%), and fluid inlet temperature. It was concluded that shell-and-tube heat exchangers have superior performance with the application of nanofluids in comparison with the base fluid. The performance has been significantly enhanced with air injection along with the nanofluids. The turbulence with air injection is a responsible factor to improve the performance of the shell-and-tube heat exchanger. Some of the authors have worked with different metal oxide nanofluids to enhance the performance of heat transfer in areas such as microelectronics, normal channel, and heat pipes and successfully optimized the performance of the nanofluids [34,35,36].

The thermal performance increased with the addition of nanoparticles for higher concentrations, and it has been improved up to 40% compared to the base fluid. Xia et al. [37] investigated the two-fluid flow heat exchanger for the entrance dissipation minimization, and in this study, three types of heat exchangers were considered in which counter heat exchanger realized the entrance minimization in the heat transfer process. A similar type of study was done by Wei et al. [38] on cross-section tube exchanger in which heat transferability of the heat exchanger was calculated with and without insertion of the fins. Some studies have done on the different heat exchangers with H, T, X, and disc-shaped heat exchanger and optimization of various parameters have been done [3, 39,40,41,42,43]. Experimental and numerical investigations [3, 44, 45] were done in case of a double-pipe heat exchanger with a variation of Reynolds number and other parameters to make it more viable toward commercial use [46]. Xie et al. [47] worked on a supercharged boiler with different parameters and observed that with an increase in an outer diameter of the heat transfer tube the complex function decreases first and then increases. Furthermore, some efforts were done to reduce the dimensionless pumping power in the evaporator [48]. Instead of using some traditional correlation to predict the thermal conductivity, a few studies [46, 49,50,51] are published with the use of an artificial neural network (ANN) and MARS which are quite close to predicting the change in the thermal conductivity of the base fluid with the introduction of nanofluids in it.

The study aims to analyze the performance and exergy analysis of a small-scale shell-and-tube heat exchanger with the air injection method. The exergy loss analysis in the horizontal heat exchanger was reported very limited. To implement this goal, the effects of air injection at different locations have been studied. Also, exergy loss analysis with air injection at different locations has been studied. The effect of air bubble injection on the number of thermal units (NTU) is investigated. The performance of the heat exchanger can be estimated with the effectiveness of the device. In this study, the shell-and-tube heat exchanger has been placed horizontally since the heat exchanger is used horizontally in most industries.

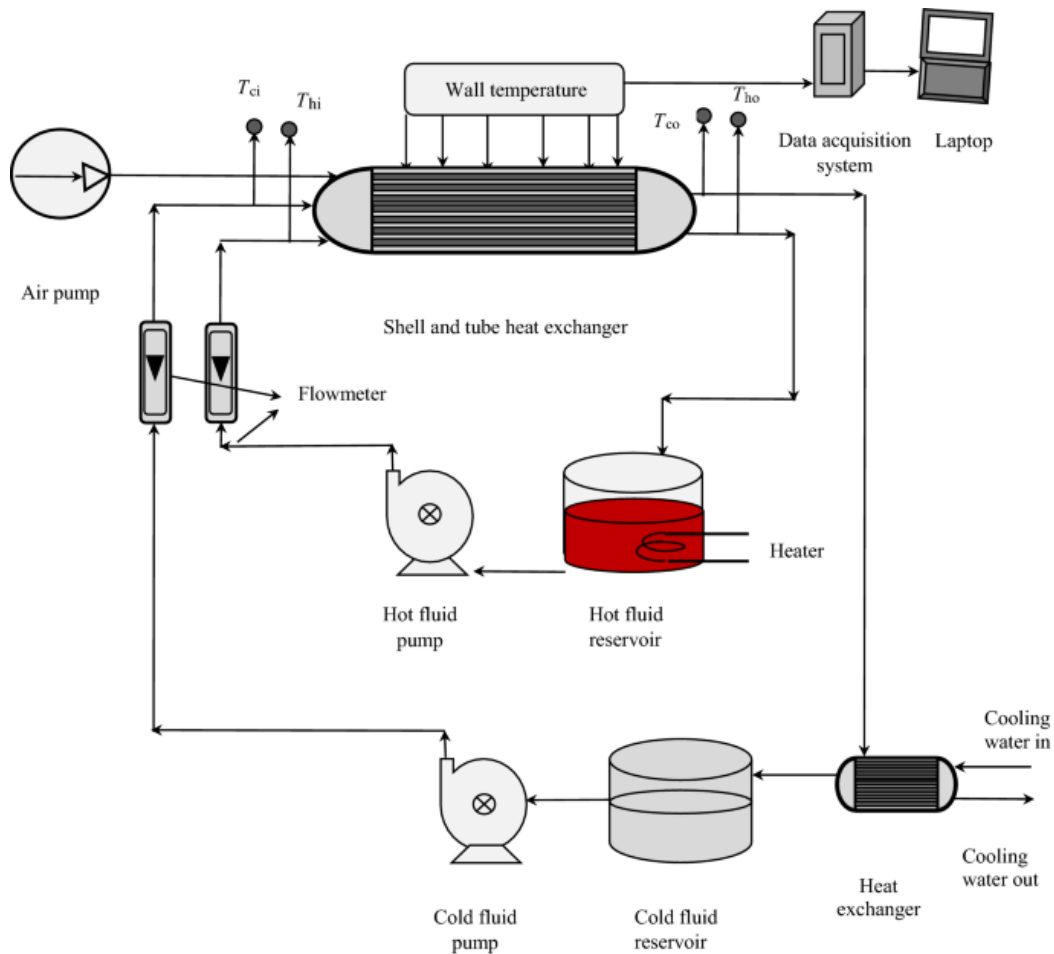


**Fig. 1.** Schematic diagram of the experimental facility

## Experimental

To analyze the performance and exergy analysis, a laboratory-scale test setup has been prepared to conduct the experimentation. The schematic diagram of the test facility has been shown in Fig. 1. In this experiment, the water is heated in a reservoir of 10-l capacity with a proportional integral differential (accuracy  $\pm 0.1$  °C) controller, and the reservoir was completely insulated to minimize the heat loss to surroundings. The test section (shell-and-tube heat exchanger) is also insulated from outside to prevent heat loss. The shell-and-tube heat exchanger consists of a shell made of mild steel with an inlet, outlet, and four straight tubes made of copper having an inlet and outlet on the same side. The shell-and-tube heat exchanger used in the experiment is similar to the AEU TEMA standards having straight tube passes. Also, the inlet and outlet of the tubes are on the same side, which consists of four passes. The leakage between the tube and the shell side has been prevented by using proper sealing. Additionally, there is a provision to clean the tubes easily by opening the head of the shell-and-tube heat exchanger. The shell has an internal diameter of about 53 mm while the tubes have internal and external diameters of about 10 mm and 12.5 mm, respectively. The tubes are arranged in a square profile. The air injection pump (accuracy

of  $\pm 0.5\%$ ) is used for injecting the air to the tube and shell side. The air pump has a capacity of  $3.5 \text{ l min}^{-1}$  and can generate a maximum pressure of  $0.02 \text{ MPa}$ . The air is injected at three different locations such as (1) inlet of the tube, (2) inlet of the shell, and (3) throughout the tube. The air is injected through a plastic tube in which small holes were provided at specified length intervals. The cold and hot fluid flows are controlled by flow meters of the accuracy of  $\pm 0.5\%$ . For measuring the temperature, thermocouples (accuracy  $\pm 0.1 \text{ }^\circ\text{C}$ ) are attached at different locations which are connected to a data logger system. The flow meters and thermocouples were calibrated before the experimentation. To minimize the variation in output reading, each experiment has been conducted three times.

## Data calculations

The overall heat transfer coefficient is calculated by using the following correlation.

$$U = \frac{Q_{\text{avg}}}{A_o \Delta T_{\text{LMTD}}} \quad (1)$$

where  $A_o$  is the tube area and  $\Delta T_{\text{LMTD}}$  is logarithmic mean temperature difference.

The logarithmic mean temperature difference is given as follows:

$$T_{\text{LMTD}} = \frac{(T_{\text{hi}} - T_{\text{ci}}) - (T_{\text{ho}} - T_{\text{co}})}{\ln \left\{ \frac{T_{\text{hi}} - T_{\text{ci}}}{T_{\text{ho}} - T_{\text{co}}} \right\}} \quad (2)$$

The heat transfer rate, heat transfer coefficient, and the Nusselt number can be obtained by using the following equations:

$$Q_{\text{avg}} = \frac{1}{2}(Q_{\text{h}} + Q_{\text{c}}) \quad (3)$$

where

$$Q_{\text{h}} = \dot{m}_{\text{h}} \times c_{\text{ph}} \times (T_{\text{h,i}} - T_{\text{h,o}}) \quad (4)$$

and

$$Q_{\text{c}} = \dot{m}_{\text{c}} \times c_{\text{pc}} \times (T_{\text{c,o}} - T_{\text{c,i}}) \quad (5)$$

The convective heat transfer coefficient and the Nusselt Number are given as follows:

$$h = \frac{Q_{\text{avg}}}{A \times (T_{\text{w}} - T_{\text{m}})} \quad (6)$$

$$\text{Nu} = \frac{h \times d_i}{k} \quad (7)$$

The (Number of Transfer Units) NTU and the effectiveness can be determined by using the following equations.

$$NTU = \frac{A_o \times U_o}{C_{\min}} \quad (8)$$

where  $C_{\min} = \text{Min} \{C_h \text{ and } C_c\}$

$$C_h = \dot{m}_h \times C_{ph} \quad (9)$$

$$C_c = \dot{m}_c \times C_{pc} \quad (10)$$

and the effectiveness is given as

$$\varepsilon = \frac{Q_{\text{avg}}}{C_{\min} \times (T_{hi} - T_{ci})} \quad (11)$$

Exergy analysis and the dimensionless exergy loss can be calculated using Akpinar and Bicer [13] study method and can be given as follows:

$$E = E_h + E_c \quad (12)$$

where

$$E_h = T_e \left\{ \dot{m}_h \times C_{ph} \times \ln \frac{T_{ho}}{T_{hi}} \right\} \quad (13)$$

$$E_c = T_e \left\{ \dot{m}_c \times C_{pc} \times \ln \frac{T_{co}}{T_{ci}} \right\} \quad (14)$$

and the dimensionless exergy loss is given as follows:

$$e = \frac{E}{T_e \times C_{\min}}. \quad (15)$$

## Results and discussions

To ensure the accuracy of the testing system, a few experiments were conducted with normal operating conditions, and the results of these experiments have been compared with Dittus–Boelter [52] equation. The validation of experimental results has been done with Dittues–Boelter [52] equation as shown in Fig. 2. There is a good agreement between the experimental and calculated results so that only 5–7% error in all operating conditions can be observed.

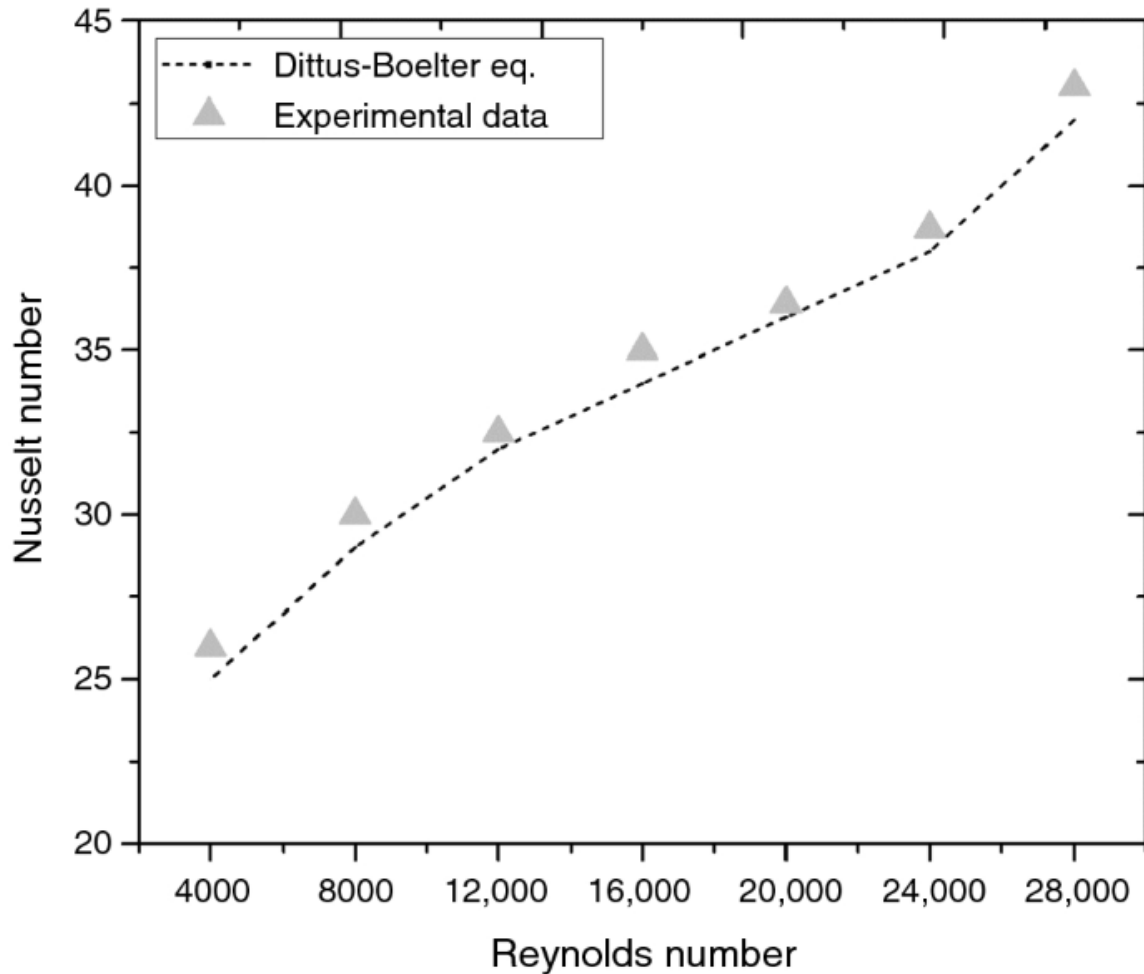


Fig. 2. Experimental results validation with theoretical results

### Heat transfer coefficient

The heat transfer coefficient is measured as the heat transfer from the fluid flows to the solid surface on which fluids are flowing. In a shell-and-tube heat exchanger, the convection occurs in two places. First, the heat from the hot water is transferred to the outer tube surface while the second is from hot water to cold water is flowing shell side. Now, this heat from the tube surface is carried away by the cooling water, thus overall process takes place. As has been observed, the flow rate affects the heat transfer rate. Similarly, with an increase in the flow rate, the heat transfer coefficient also increases in all cases, as shown in Fig. 3. Furthermore, injecting the air bubbles in the flowing water enhances the heat transfer coefficient. It has been observed that injecting air bubbles throughout the tube section showed a minimum heat transfer coefficient of about  $337 \text{ (W m}^{-2} \text{ K}^{-1}\text{)}$  which corresponds to 49% with respect to without air injection. As the air is injected throughout the tube, it creates more bubbles in the fluids which further creates more turbulence in the fluid. The turbulences of fluids alter the regime and augmentation of the heat transfer coefficient. The constant flow rate occurred in the shell side when the air was injected on the shell side. The mean velocity of the fluid is also increased with air injection. While the maximum heat transfer is around  $869 \text{ (W m}^{-2} \text{ K}^{-1}\text{)}$  which corresponds to 41% contributed to the case



without air injection system at hot water temperature that is at 40 °C at different ranges of Reynolds number. The minimum heat transfer coefficient in the air injection at the shell side without air injection is 264.45 ( $\text{W m}^{-2} \text{K}^{-1}$ ) which corresponds to 23% while the maximum value obtained is 786.62 ( $\text{W m}^{-2} \text{K}^{-1}$ ) at 50 °C and 841 ( $\text{W m}^{-2} \text{K}^{-1}$ ) at 70 °C for different ranges of Reynolds number.

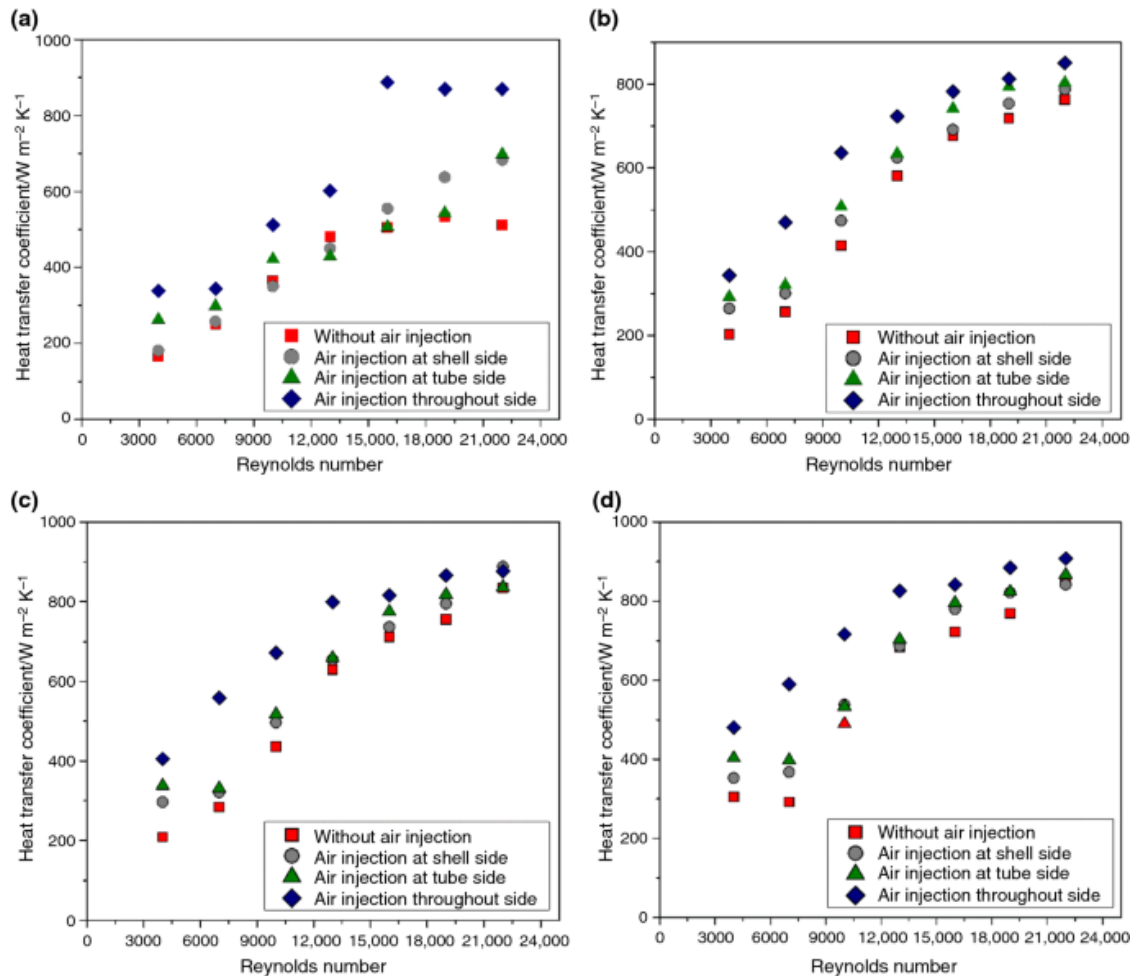


**Fig. 3.** Heat transfer coefficient under different air injection methods for fluid temperature **a** 40 °C, **b** 50 °C, **c** 60 °C and **d** 70 °C

Similarly, the minimum heat transfer coefficient in air injection at the tube inlet side without air injection is 403 ( $\text{W m}^{-2} \text{K}^{-1}$ ), which corresponds to 24%. As the air is injected in the tube side, it alters the thermal boundary layer and enhances the Reynolds number. It has been observed that the impact of the air bubbles at higher Reynolds is more as compared to the low Reynolds number. On the other hand, the obtained maximum value is 866 ( $\text{W m}^{-2} \text{K}^{-1}$ ) at 60 °C at different ranges of the Reynolds number. The maximum heat transfer coefficient is measured to be 907 ( $\text{W m}^{-2} \text{K}^{-1}$ ) at 70 °C for the Reynolds number of 22,000 as the air has been injected throughout the tube. The more number of holes in the throughout tube method creates more bubbles which leads to more heat transfer. It has been concluded that injecting the air bubble leads to an increase in the turbulence of the flowing fluid. This increase in the turbulence enhances the heat transfer rate.

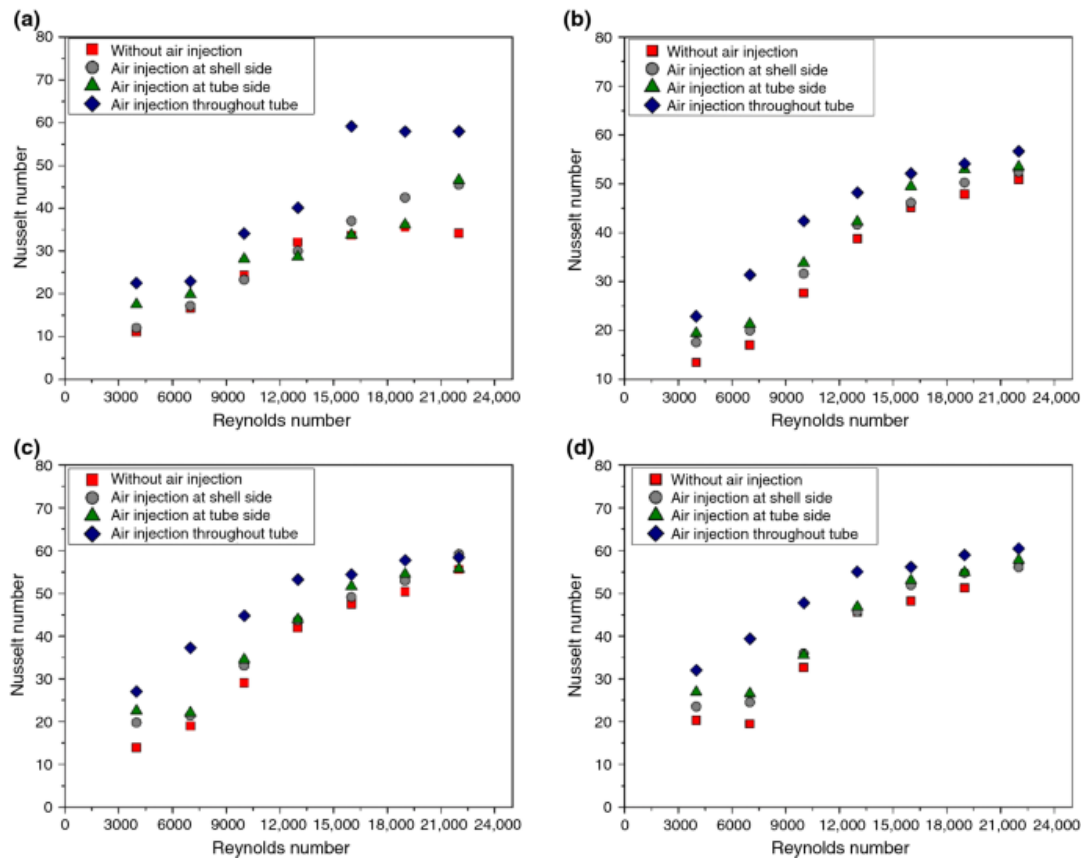


**Fig. 4.** Variation of Nusselt number with Reynolds number under different air injection methods for fluid temperature **a** 40 °C, **b** 50 °C, **c** 60 °C and **d** 70 °C

### Nusselt number

Nusselt number is one of the most important parameters which determines the convection rate and the performance of heat exchangers. With an increase in the flow rate of the hot water, an improvement in the Nusselt number has been observed due to a rise in the heat transfer rate. From Fig. 4, it has been observed that the maximum Nusselt number is obtained at a higher flow rate or the higher Reynolds number. Hence, Nusselt number can be stated as a function of Reynolds Number. As the air bubbles are injected at different points, it starts to move in the upward direction, which creates turbulence in the flow rate, then this turbulence improves the heat transfer rate. Apart from this, the effect on the thermal boundary layer also leads to a heat transfer augmentation, and the bubble flow regime also has some effects which alter the turbulence of the fluid which is flowing inside the tubes. These are some reasons which can be mentioned that lead to the augmentation of the heat transfer capacity. With the injection of air at different points in the shell-and-tube heat exchanger, an enhancement in the Nusselt number has been observed at different flow rates and temperatures. It can be mentioned that injecting air bubbles throughout the tube section shows that the minimum enhancement in the Nusselt number was 13.81% without air injection, while the obtained Nusselt number is around 37.37 which corresponds to 15.62% without air injection at a maximum hot water temperature of 70 °C at different ranges of Reynolds Number. The minimum Nusselt number in the tube side air injection without air injection was higher than 8.81%. On the other hand, the maximum was

9.37% at 70 °C at different ranges of Reynolds Number. Similarly, the Nusselt number in the shell-side air injection without using air injection was higher, which was about 5.45%, while the maximum value was 6.25% at 70 °C and different ranges of the Reynolds Number. Additionally, similar enhancements have been observed at other temperatures.

The Nusselt number in the present has similar trends with the work of Pourhedyat et al. [23], and it has good agreement with the published work. An enhancement has been observed due to the motion of the bubbles, which creates extra turbulence which enhances the heat transfer rate; ultimately, it results in improving the Nusselt number. It has been observed that by using the air injection method throughout the tube, the enhancement in Nusselt number is more than that of the air injection at either shell entrance or the tube entrance.

### **Effectiveness**

Effectiveness is the change in the fluid temperature with a smaller capacity rate to the maximum possible temperature difference in the heat exchangers. It indicates the performance of a heat exchanger and how much the heat exchanger is effective for a specific purpose. The effectiveness depends on the actual heat transfer rate and the maximum possible heat transfer rate.

The heat transfer rate depends on the mass flow rate of the fluid; thus, the flow rate affects the effectiveness of the heat exchanger. Figure 5 shows the effect of flow rate on the effectiveness of the shell-and-tube heat exchanger. Maximum effectiveness has been obtained at a maximum flow rate or maximum Reynolds number. As the heat transfer rate increases with the air injection, the effectiveness also enhances. Through the experimental analysis, it has been observed that injecting air bubbles throughout the tube section shows minimum effectiveness of about 0.3337 which corresponds to 14% without air injection while the maximum effectiveness is around 0.416 which corresponds to 17% without air injection at a maximum hot water temperature of 70 °C at different ranges of Reynolds number. The minimum effectiveness in air injected at the shell side without air injection is 0.2981 which corresponds to 3%. On the other hand, the maximum value is 0.366 which corresponds to 6% at 70 °C at different ranges of Reynolds Number. Similarly, the minimum effectiveness in air injected at the tube side without air injection is 0.321 which corresponds to 11% while the maximum value is 0.389 which corresponds to 14% at 60 °C and different range of the Reynolds number. Additionally, a similar trend has been observed with other temperatures. The obtained results at different temperatures and flow rate conditions at different air injection conditions have been shown in Fig. 5. It has been observed that the present work has quite similar trends with the work of Heyhat et al. [22] as some operations are different in both works (Table 1).

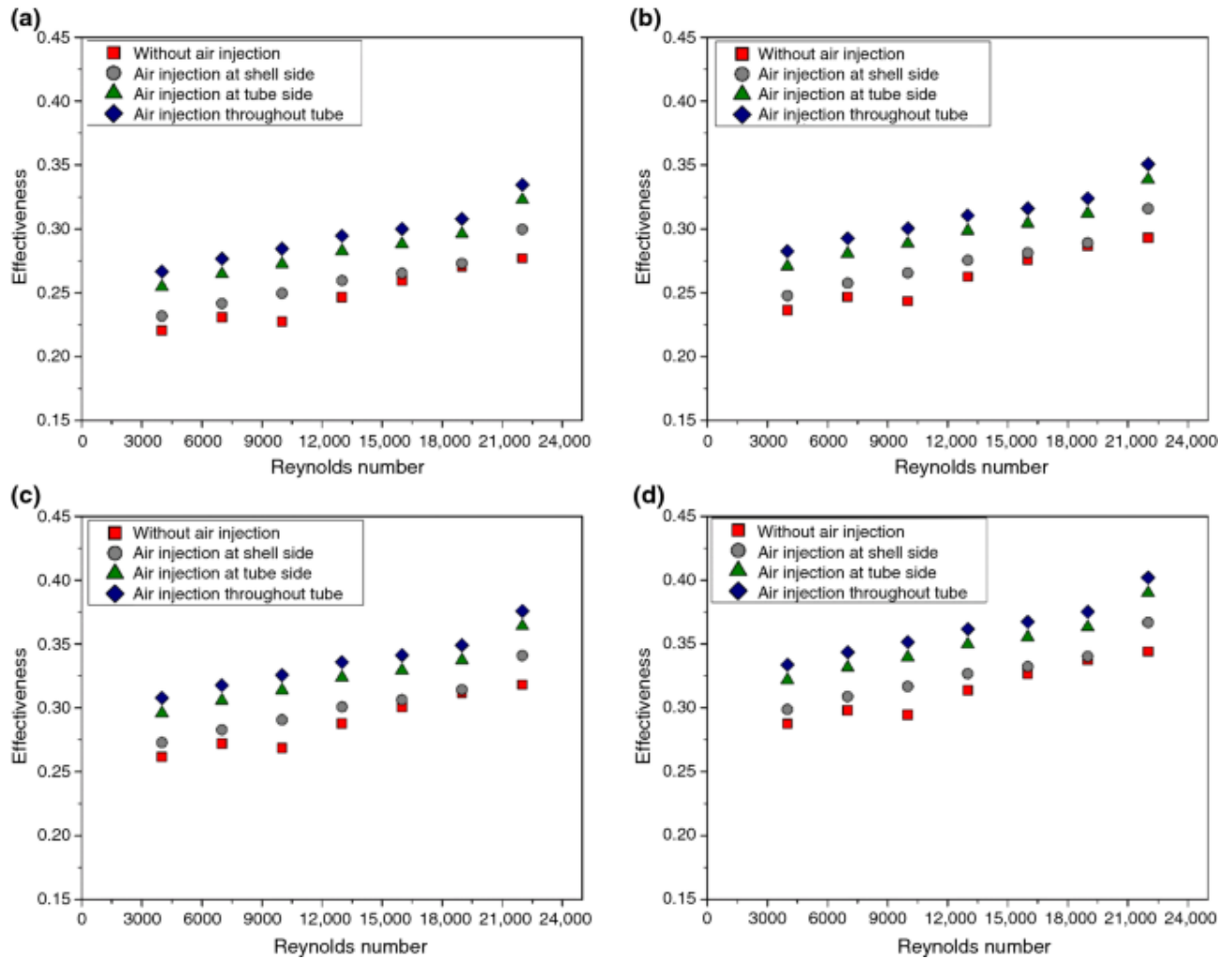


**Fig. 5.** Effectiveness of the heat exchanger under different air injection methods for fluid temperature **a** 40 °C, **b** 50 °C, **c** 60 °C and **d** 70 °C

**Table 1** Parametric conditions

S. No	Parameters	Range
1	Reynolds number	4000–22,000
2	Fluid temperature/°C	40–70
3	Air injection	1. Without air injection 2. Air injection at shell side 3. Air injection at tube side 4. Air injection throughout the tube

### Exergy loss

Exergy is the thermodynamic property defined as the maximum amount of the useful work that can be achieved from a reversible system in a specific environment. It is one of the important parameters when any actual device is compared with a real device. In heat exchangers, the exergy gained by one fluid is compared with the exergy given out by

another fluid. A temperature difference is one of the major causes of the losses in heat exchangers. It has been observed from the experimental result that exergy loss and dimensionless exergy loss increase with a rise in flow rate, which has been shown in Fig. 6. Maximum exergy loss is obtained at a maximum flow rate of  $3.5 \text{ l m}^{-1}$  for the hot fluid and cold fluid side, and similarly, the dimensionless exergy loss, which is based upon the exergy of the sum of hot fluid and cold fluid side with respect to maximum work is also increasing with air injection as compared to the without air injection in heat exchanger under the same operating conditions.

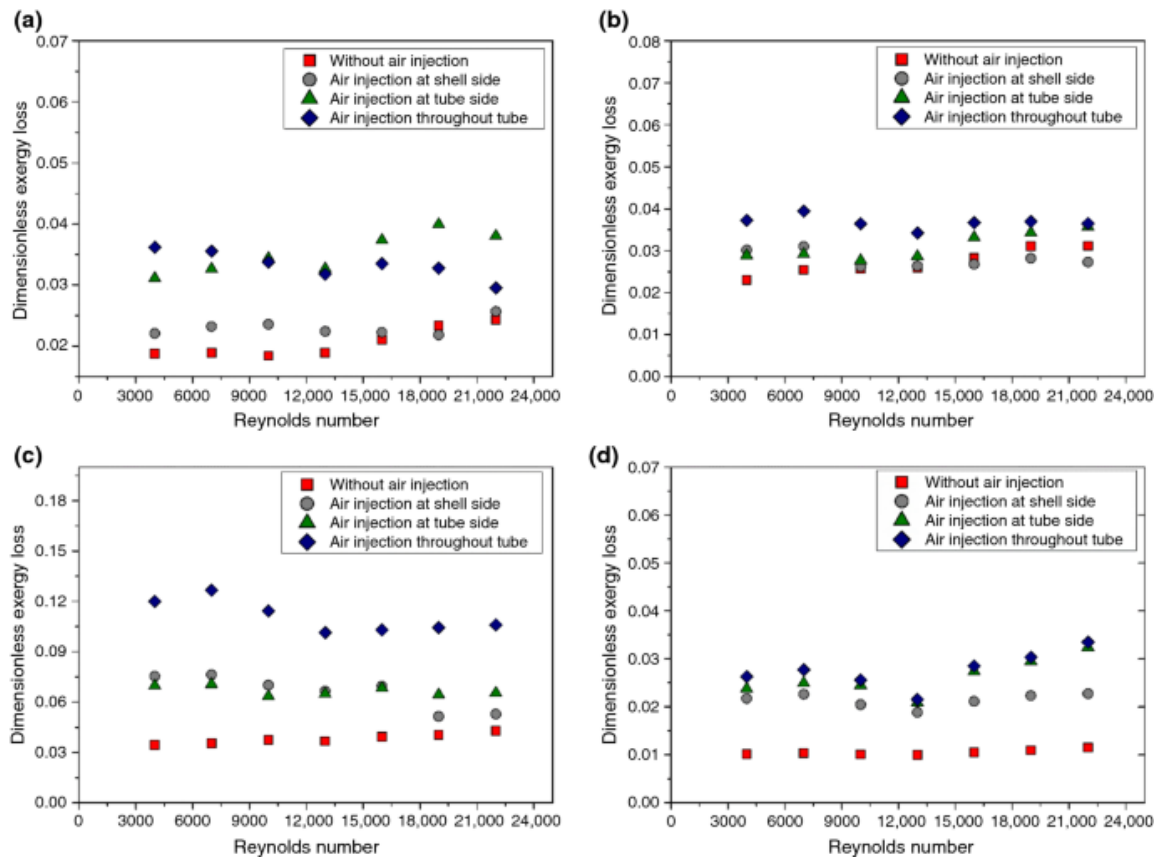


**Fig. 6.** Dimensionless exergy loss at different air injection methods for fluid temperature **a** 40 °C, **b** 50 °C, **c** 60 °C and **d** 70 °C

The increase in the flow rate leads to a rise in the temperature difference. As a result, the exergy loss and the dimensionless exergy loss augment. With the air bubble injection in the heat exchanger, it has been observed that the temperature difference increases, which leads to an increase in the exergy loss. Additionally, the increment in exergy loss results in augmenting the dimensionless exergy loss. It can be stated which injecting air bubbles throughout the tube section show minimum dimensionless exergy coefficient of about 0.03241 which corresponds to 27.49% with no air injection in the tube while the maximum exergy loss is around 0.03569 which related to 31.02% with no air injection at a maximum hot water temperature of 70 °C at different ranges of Reynolds number. The minimum exergy loss in the air at the shell side concerning no air obtained is 0.02601 which corresponds to 2.32% while the maximum value obtained is 0.02801 which corresponds to 3.01% at 60 °C at a different range of Reynolds number. Similarly, the minimum

dimensionless exergy loss for air at tube inlet with respect to no air injection is 0.02721 which corresponds to 7.04% while the maximum value is 0.0302 which corresponds to 10.86% at 60 °C and different range of the Reynolds number. A similar trend has been observed for other temperatures. The work has been carried out on a small-scale shell-and-tube heat exchanger with the air injection technique to measure the performance and exergy analysis. In the research, different air injection methods are suggested, and their effect has been analyzed. The air injection technique is a good promising method as compared to other conventional methods, i.e., use of turbulators, inserts, to improve the performance of the heat exchanger because this technique has low exergy loss as compared to other methods.

## Conclusions

In this research, the performance and exergy loss in a shell-and-tube heat exchanger has been calculated. The effect of air injection in the flowing fluid has been analyzed by injecting air at the shell side, tube side, and throughout the tube. Finally, the obtained results have been compared to the case without air injection. The air injection technique is one of the promising techniques to improve the performance of heat exchangers. Among the three different cases, the air injection throughout the tube is more effective followed by air injection in tube inlet and shell side air injection. The maximum heat transfer coefficient was observed approximately 41% when air injected throughout the tube as compared to the no air injection in the shell and tube side. With injecting air bubbles throughout the tube section, enhancement in the Nusselt number was 13–25% for the case without air injection at a maximum hot water temperature of 70 °C. Maximum effectiveness has been obtained at a maximum flow rate or maximum Reynolds number. As the heat transfer rate increases with the air injection, the effectiveness also enhances. The exergy loss has been increased by introducing air injection in all cases, i.e., injection of air at (a) shell side, (b) tube side, and throughout the tube. The injecting air bubbles throughout the tube section show minimum dimensionless exergy which is 27.49% for no air injection while the maximum is around 31.02% for no air injection at the maximum hot water temperature of 70 °C.

## References

1. Maddah H, Ghazvini M, Ahmadi MH. Predicting the efficiency of CuO/water nanofluid in heat pipe heat exchanger using neural network. *Int Commun Heat Mass Transf.* 2019;104:33–40.
2. Ahmadi MH, Ghazvini M, Maddah H, Kahani M, Pourfarhang S, Pourfarhang A, et al. Prediction of the pressure drop for CuO/(ethylene glycol–water) nanofluid flows in the car radiator by means of Artificial Neural Networks analysis integrated with genetic algorithm. *Phys A Stat Mech its Appl.* 2020;124008.
3. Aghayari R, Maddah H, Pourkiaei SM, Ahmadi MH, Chen L, Ghazvini M. Theoretical and experimental studies of heat transfer in a double-pipe heat exchanger equipped with twisted tape and nanofluid. *Eur Phys J Plus.* 2020. <https://doi.org/10.1140/epjp/s13360-020-00252-8>.

4. Ahmadlouydarab M, Ebadolahzadeh M, Muhammad H. Effects of utilizing nanofluid as working fluid in a lab-scale designed FPSC to improve thermal absorption and efficiency. *Physica A*. 2020;540:123109. <https://doi.org/10.1016/j.physa.2019.123109>.
5. Muneeshwaran M, Sajjad U, Ahmed T, Amer M, Wang C. Performance improvement of photovoltaic modules via temperature homogeneity improvement. 2020;203.
6. Ali HM. Recent advancements in PV cooling and efficiency enhancement integrating phase change materials based systems – A comprehensive review. *Sol Energy*. 2020;197:163–98. <https://doi.org/10.1016/j.solener.2019.11.075>.
7. Tariq SL, Ali HM, Akram MA, Mansoor M, Ahmadlouydarab M. Nanoparticles enhanced phase change materials (NePCMs) -A recent review. *Appl Therm Eng*. 2020;176:115305. <https://doi.org/10.1016/j.applthermaleng.2020.115305>.
8. Abbas F, Raza T, Babar H, Mansoor M, Sajjad U, Amer M. Nano fluid : potential evaluation in automotive radiator. 2020;297.
9. Ghazvini M, Maddah H, Peymanfar R, Ahmadi MH, Kumar R. Experimental evaluation and artificial neural network modeling of thermal conductivity of water based nanofluid containing magnetic copper nanoparticles. *Phys A Stat Mech Appl*; 2020;124127.
10. Ahmadi MH, Baghban A, Ghazvini M, Hadipoor M, Ghasempour R, Nazemzadegan MR. An insight into the prediction of TiO<sub>2</sub>/water nanofluid viscosity through intelligence schemes. *J Therm Anal Calorim*. 2019;139:2381–94.
11. Ahmadi MH, Tatar A, Seifaddini P, Ghazvini M, Ghasempour R, Sheremet MA. Thermal conductivity and dynamic viscosity modeling of Fe<sub>2</sub>O<sub>3</sub>/water nanofluid by applying various connectionist approaches. *Numer Heat Transf A Appl*. 2018;74:1301–22.
12. Ahmadi MH, Ghazvini M, Maddah H, Kahani M, Pourfarhang S, Pourfarhang A, et al. Prediction of the pressure drop for CuO/(Ethylene glycol–water) nanofluid flows in the car radiator by means of Artificial Neural Networks analysis integrated with genetic algorithm. *Phys A Stat Mech Appl*. 2020;546: 124008.
13. Ahmadi MH, Baghban A, Sadeghzadeh M, Hadipoor M, Ghazvini M. Evolving connectionist approaches to compute thermal conductivity of TiO<sub>2</sub>/water nanofluid. *Phys A Stat Mech Appl*. 2019
14. Abbasian Arani AA, Amani J. Experimental investigation of diameter effect on heat transfer performance and pressure drop of TiO<sub>2</sub>-water nanofluid. *Exp Therm Fluid Sci*. 2013;44: 520–533.
15. Heyhat MM, Kowsary F, Rashidi AM, Alem Varzane Esfehiani S, Amrollahi A. Experimental investigation of turbulent flow and convective heat transfer characteristics of alumina water nanofluids in fully developed flow regime. *Int Commun Heat Mass Transf*. 2012;39: 1272–1278.

16. Singh G, Gangacharyulu D, Bulasara VK. Experimental investigation of the effect of heat transfer and pressure drop on performance of a flat tube by using water-based Al<sub>2</sub>O<sub>3</sub> nanofluids. *Int J Energy Clean Environ.* 2018;19: 1–17.
17. Sokhal GS, Gangacharyulu D, Bulasara VK. Heat transfer and pressure drop performance of alumina–water nanofluid in a flat vertical tube of a radiator. *Chem Eng Commun.* 2018;205: 257–68.
18. Arabia S. In tube convection heat transfer enhancement: SiO<sub>2</sub> aqua based nano fluids. 2020;308.
19. Lu J, Fernández A, Tryggvason G. The effect of bubbles on the wall drag in a turbulent channel flow. *Phys Fluids.* 2005;17: 1–12.
20. Mattson M, Mahesh K. Simulation of bubble migration in a turbulent boundary layer. *Phys Fluids.* 2011;23: 1–13.
21. Jacob B, Olivieri A, Miozzi M, Campana EF, Piva R. Drag reduction by microbubbles in a turbulent boundary layer. *Phys Fluids.* 2010;22.
22. Mahdi Heyhat M, Abdi A, Jafar zad A. Performance evaluation and exergy analysis of a double pipe heat exchanger under air bubble injection. *Appl Therm Eng.* 2018;143: 582–593.
23. Pourhedayat S, Sadighi Dizaji H, Jafarmadar S. Thermal-exergetic behavior of a vertical double-tube heat exchanger with bubble injection. *Exp Heat Transf.* 2019;32: 455–468.
24. Sadighi Dizaji H, Jafarmadar S, Abbasalizadeh M, Khorasani S. Experiments on air bubbles injection into a vertical shell and coiled tube heat exchanger; exergy and NTU analysis. *Energy Convers Manag.* 2015;103: 973–80.
25. Winkel ES, Ceccio SL, Dowling DR, Perlin M. Bubble-size distributions produced by wall injection of air into flowing freshwater, saltwater and surfactant solutions. *Exp Fluids.* 2004;37: 802–810.
26. Ramezanizadeh M, Alhuyi Nazari M, Ahmadi MH, Açikkalp E. Application of nanofluids in thermosyphons: a review. *J Mol Liq.* 2018;272: 395–402.
27. Khorasani S, Dadvand A. Effect of air bubble injection on the performance of a horizontal helical shell and coiled tube heat exchanger: an experimental study. *Appl Therm Eng.* 2017;111: 676–683.
28. Ahmadi AA, Arabbeiki M, Ali HM, Goodarzi M. Configuration and optimization of a minichannel using water – alumina nanofluid by non-dominated sorting genetic algorithm and response surface method. 2020;1–22.
29. Akpınar EK, Bicer Y. Investigation of heat transfer and exergy loss in a concentric double pipe exchanger equipped with swirl generators. *Int J Therm Sci.* 2005;44: 598–607.



30. Nandan A, Singh G. Experimental studies on heat transfer performance of shell and tube heat exchanger with air bubble injection. *Indian J Sci Technol.* 2016;9.
31. Nandan A, Singh G. Experimental study of heat transfer rate in a shell and tube heat exchanger with air bubble injection. *Int J Eng Trans B Appl.* 2016;29: 1160–1166.
32. Thakur G, Singh G, Thakur M, Kajla S. An experimental study of nanofluids operated shell and tube heat exchanger with air bubble injection. *Int J Eng Trans A Basics.* 2018;31: 136–143.
33. Thakur G, Singh G. An experimental investigation of heat transfer characteristics of water based  $\text{Al}_2\text{O}_3$  nanofluid operated shell and tube heat exchanger with air bubble injection technique. *Int J Eng Technol.* 2017;6: 83–90.
34. Tariq HA, Anwar M, Malik A, Ali HM. Hydro-thermal performance of normal-channel facile heat sink using  $\text{TiO}_2\text{-H}_2\text{O}$  mixture (Rutile–Anatase) nanofluids for microprocessor cooling. *J Therm Anal Calorim.* 2020. <https://doi.org/10.1007/s10973-020-09838-x>.
35. Khalid SU, Babar H, Ali HM, Janjua MM, Ali MA. Heat pipes: progress in thermal performance enhancement for microelectronics. *J Therm Anal Calorim.* 2020. <https://doi.org/10.1007/s10973-020-09820-7>.
36. Sriharan G, Harikrishnan S, Ali HM. Experimental investigation on the effectiveness of MHTHS using different metal oxide-based nanofluids. *J Therm Anal Calorim.* 2020. <https://doi.org/10.1007/s10973-020-09779-5>.
37. Xia SJ, Chen LG, Sun FR. Optimization for entransy dissipation minimization in heat exchanger. *Chin Sci Bull.* 2009;54: 3587–3595.
38. Wei S, Chen L, Sun F. Constructal entransy dissipation minimization of round tube heat exchanger cross-section. *Int J Therm Sci.* 2011;50: 1285–1292. <https://doi.org/10.1016/j.ijthermalsci.2011.02.025>.
39. Feng HJ, Chen LG, Xie ZH, Sun FR. Constructal optimization for H-shaped multi-scale heat exchanger based on entransy theory. *Sci China Technol Sci.* 2013;56: 299–307.
40. Chen L, Feng H, Xie Z, Sun F. Thermal efficiency maximization for H- and X-shaped heat exchangers based on constructal theory. *Appl Therm Eng.* 2015;91: 456–462. <https://doi.org/10.1016/j.applthermaleng.2015.08.029>.
41. Feng H, Chen L, Xia S. Constructal design for disc-shaped heat exchanger with maximum thermal efficiency. *Int J Heat Mass Transf.* 2019;130: 740–746. <https://doi.org/10.1016/j.ijheatmasstransfer.2018.11.003>.
42. Feng H, Chen L, Wu Z, Xie Z. Constructal design of a shell-and-tube heat exchanger for organic fluid evaporation process. *Int J Heat Mass Transf.* 2019;131: 750–756. <https://doi.org/10.1016/j.ijheatmasstransfer.2018.11.105>.

43. Feng H, Xie Z, Chen L, Wu Z, Xia S. Constructal design for supercharged boiler superheater. *Energy*. 2020;191: 116484. <https://doi.org/10.1016/j.energy.2019.116484>.
44. Nasirzadehroshenin F, Sadeghzadeh M, Khadang A, Maddah H, Ahmadi MH, Sakhaeinia H, et al. Modeling of heat transfer performance of carbon nanotube nanofluid in a tube with fixed wall temperature by using ANN-GA. *Eur Phys J Plus*. 2020. <https://doi.org/10.1140/epjp/s13360-020-00208-y>.
45. Shamsavar A, Ali HM, Mahani RB, Talebizadehsardari P. Numerical study of melting and solidification in a wavy double-pipe latent heat thermal energy storage system. *J Therm Anal Calorim*. 2020. <https://doi.org/10.1007/s10973-020-09864-9>.
46. Ramezanizadeh M, Nazari MA, Hossein M. Mechanics experimental and numerical analysis of a nanofluidic thermosyphon heat exchanger. 2019;2060. <https://doi.org/10.1080/19942060.2018.1518272>.
47. Xie Z, Feng H, Chen L, Wu Z. Constructal design for supercharged boiler evaporator. *Int J Heat Mass Transf*. 2019;138: 571–579.
48. Wu Z, Feng H, Chen L, Xie Z, Cai C. Pumping power minimization of an evaporator in ocean thermal energy conversion system based on constructal theory. *Energy*. 2019;181: 974–84. <https://doi.org/10.1016/j.energy.2019.05.216>.
49. Ramezanizadeh M, Nazari MA. Modeling thermal conductivity of Ag/water nanofluid by applying a mathematical correlation and artificial neural network. 2019;468–474.
50. Komeilibirjandi A, Hossein A, Akbar R. Thermal conductivity prediction of nanofluids containing CuO nanoparticles by using correlation and artificial neural network. *J Therm Anal Calorim*. 2019. <https://doi.org/10.1007/s10973-019-08838-w>.
51. Maleki A, Elahi M, El M, Assad H, Alhuyi M, Mostafa N, et al. Thermal conductivity modeling of nanofluids with ZnO particles by using approaches based on artificial neural network and MARS. *J Therm Anal Calorim*. 2020. <https://doi.org/10.1007/s10973-020-09373-9>.
52. Dittus FW, Boelter LMK. Heat transfer in automobile radiators of the tubular type. *Int Commun Heat Mass Transf*. 1985; 12:3–22.